International Journal of Engineering Trends and Technology
ISSN: 2231–5381 / https://doi.org/10.14445/22315381/IJETT-V73I9P117

Volume 73 Issue 9, 194-201, September 2025

Original Article

A Study on the Response Characteristics of a Smart Seismic Isolation Device under Earthquake Excitation

Yu-Jin Jeong[1], Min-Woo Kim[1], Dong-Hwan Lee[2], Hyoung-Woo Lee[3]

[1]*Department of Mechanical Engineering, Jungwon University, Republic of Korea, Chungbuk.*
[2]*Earthquake Intelligence Services Co., Ltd., Republic of Korea, Daejeon.*
[3]*Department of Unmanned Aeromechanical Engineering, Jungwon University, Republic of Korea, Chungbuk.*

[3]*Corresponding Author : leehwoo@jwu.ac.kr*

Received: 21 April 2025 Revised: 05 September 2025 Accepted: 15 September 2025 Published: 30 September 2025

Abstract - *During earthquakes, damage to Non-Structural Components (NSCs) inside buildings can cause critical system failure and human casualties, emphasizing the growing need for protective measures. In particular, if damaged, key equipment like telecommunication cabinets-though not structural-can lead to significant social and economic losses, requiring advanced vibration isolation technology. This study proposes a smart seismic isolation device for protecting non-structural components. Traditional base isolation systems mainly target entire structures and have limitations in controlling residual vibrations that occur above the natural frequency. The smart isolation device combines an LM guide-based isolation structure with an MR damper, allowing dynamic response control under external excitation. Finite Element Analysis (FEA) is performed to analyze vibration response characteristics with and without isolation and under varying damping ratios. The vibration reduction performance for indoor equipment is evaluated. This study suggests the applicability of smart seismic technology and its potential contribution to enhancing seismic performance in disaster response systems and securing the stability of critical NSCs.*

Keywords - *Seismic isolation technology, Smart isolation device, LM guide, MR damper, Vibration isolation.*

1. Introduction

Seismic isolation technology reduces structural damage by effectively interrupting vibrations between the ground and structures. It is widely used as a countermeasure against earthquakes. Isolation devices absorb or disperse seismic vibrations before they reach the structure, increasing the natural period and reducing the applied forces to secure stability. This concept is not limited to exterior structural elements; it can also be applied to indoor equipment such as telecommunication cabinets. Damage to NSCs can result in severe economic loss and disrupt post-earthquake recovery [1]. A common solution for protecting indoor NSCs is the use of seismic isolation tables, often implemented using systems such as the Friction Pendulum System (FPS) or Linear Motion (LM) Guide. However, even sophisticated isolation tables cannot completely block seismic energy, and residual vibrations may be transmitted to the upper part of the structures. When residual vibrations are amplified at specific frequencies or interfere with the function of critical devices, they can cause communication outages or power loss, resulting in secondary disasters [2]. For example, during the 1995 Hanshin-Awaji Earthquake in Japan, museums, exhibition halls, and hospitals reported toppling and destruction of high-value items and equipment due to vibrations [3]. This emphasized the need for seismic isolation for internal equipment. Though such equipment may not suffer direct structural failure, it can cause secondary issues through tipping or breakage, necessitating dedicated vibration mitigation strategies. Recently, Magneto-Rheological (MR) control technology, which can respond actively to residual vibrations, has gained attention. This allows enhanced vibration control performance and is categorized as a smart isolation device. These devices respond in real time based on the vibration characteristics. Researchers have employed various approaches in the study of Seismic isolation technology. For instance, Hyun-Su Kim et al. proposed a numerical model for a hybrid system combining an MR damper with an FPS, usable at the design stage [4]. Mahdi Abdeddaim et al. applied an MR damper base isolation system considering soil-structure interaction across three soil types [5]. M.D. Christie et al. designed and modeled an MR-based pendulum tuned mass damper (MR-PTMD), verifying its ability to suppress seismic vibrations in a five-story structure [6]. Young-Soo Chun et al. proposed a hybrid isolation system using sliding bearings and lead rubber bearings to enhance performance [7]. Yerik T. Bessimbayev et al. proposed a geotechnical seismic isolation method for the protection of architectural monuments by utilizing the physical and mechanical properties of soil [8]. Pan Liu et al. introduced a Hybrid Seismic Isolation Bearing System (HSIBS), consisting

of sliding friction bearings and elastic bearings. The specimen in this study was designed based on a 30 m-span continuous reinforced concrete bridge pier, and the HSIBS was shown to enhance seismic performance by separating vertical load-bearing capacity from horizontal seismic resistance [9]. Chieh-Yu Liu et al. proposed a probabilistic design approach for an isolation system incorporating geometrically nonlinear viscous dampers under non-stationary earthquakes [10].

Furthermore, Yiyang Wei et al. developed a novel composite three-dimensional isolation bearing to overcome the drawbacks of conventional composite bearings, which typically exhibit high vertical stiffness and limited deformation capacity. This system provides both horizontal and vertical isolation and, through structural analysis of a six-story building, demonstrated improved structural safety [11]. Most of the proposed isolation devices have been designed for entire structures and therefore have limitations in protecting non-structural components. In particular, previous studies have rarely addressed the combination of an LM guide-based isolation structure with an MR damper, which is presented as a major distinguishing feature of this research. This study proposes a smart isolation system combining an LM guide-based isolation table with an MR damper as a means of overcoming existing limitations, and aims to analyze its vibration reduction effect for critical non-structural components such as a telecommunication cabinet.

2. Structural Analysis of High-Speed Coupling

2.1. Finite Element Analysis Overview

To analyze the vibration reduction performance of the isolation table, three models were created: one without an isolation system, one with an LM guide, and one with both an LM guide and an MR damper. Finite Element Analysis (FEA), which divides complex structures into elements and numerically computes dynamic behavior, was used. The models are as shown in Figure 1: (a) cabinet-only model, (b) cabinet with LM guide table, and (c) cabinet with LM guide and MR damper table.

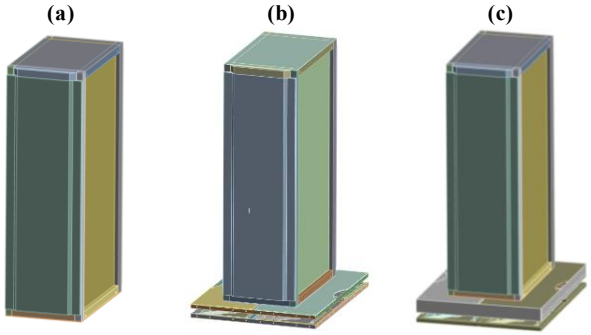

Fig. 1 Structural models for analysis (a) Cabinet, (b) Cabinet & LM guide table, and (c) Cabinet & LM guide & MR damper table.

Models were built using ANSYS 2024 R1. The cabinet-only model comprised 574,845 nodes and 103,118 elements. The LM guide model included 1,532,097 nodes and 459,687 elements, and the LM guide + MR damper model consisted of 1,718,870 nodes and 571,010 elements. The three FE models are presented in Figure 2.

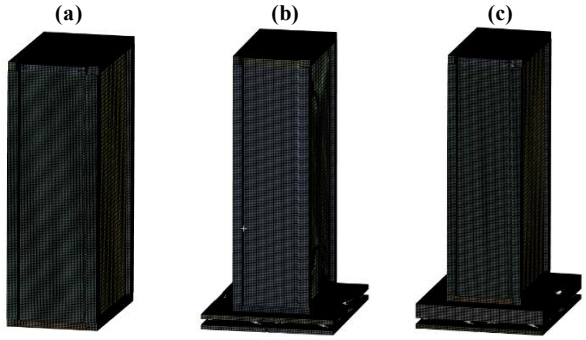

Fig. 2 Finite element analysis models (a) Cabinet, (b) Cabinet & LM guide table, and (c) Cabinet & LM guide & MR damper table.

An analysis environment closely resembling the actual system was established by reflecting each condition's geometric and structural differences. The cabinet used Hex dominant elements, while the isolation table, due to geometric complexity, used a hybrid of Hex dominant and Tetrahedron elements. A uniform mesh size of 5–10 mm was applied for reliability. To validate model accuracy, the modeled weights were compared with actual measurements. The cabinet weighed 300 kg (135 kg body + 165 kg dummy weight), and the modeled weight was 300.68 kg-an error of 0.23% (Figure 5). The LM guide isolation table weighed 50 kg, yielding a combined model weight of 350.6 kg. The LM guide + MR damper assembly weighed 200 kg, resulting in a total model weight of 500.46 kg (Figure 6).

The measured weights and the weights derived from the finite element models for each case showed a high degree of agreement, indicating that the finite element models developed in this study accurately represent the physical characteristics of the real system. The material properties used in this study are listed in Table 1.

Table 1. Material properties of SS400

Properties	Symbol	Unit	Value
Elastic Modulus	E	MPa	190
Poisson's Ratio	v	-	0.3
Density	ρ	Kg/m^3	7860

2.2. Boundary Conditions

In all analysis cases, the base was fixed using M12 bolts, and the boundary conditions were established with consideration of the self-weight. The setup was configured so as not to exceed the allowable load, reflecting the mechanical properties of the bolts and the fastening design criteria. Excitation was applied to the underside of the isolation table to transmit vibration, and the boundary conditions were configured accordingly to enable analysis of the cabinet's

dynamic behavior-particularly its natural frequency and response characteristics.

Table 2. Excitation levels according to the input frequency range

Frequency	Level	Note
1~2Hz	$x_{peak} = 0.0062m\ (6.2mm)$	$f_{cross} = \frac{1}{2\pi}\sqrt{\frac{\ddot{x}_{peak}}{x_{peak}}}$
2~35Hz	$\ddot{x}_{peak} = 0.1g\ (0.981m/s^2)$	

$$f = 1Hz, x_{peak} = 0.0062m \quad a_1 = (2\pi \times 1)^2 \times 0.0062 \quad a_1 = 0.244766m/s^2$$

$$f = 2Hz, x_{peak} = 0.0062m \quad a_1 = (2\pi \times 2)^2 \times 0.0062 \quad a_1 = 0.979065m/s^2 \quad (1)$$

The response range for all analysis cases was set between 1 and 35 Hz, corresponding to the Required Response Spectrum (RRS) specified by the National Radio Research Agency (NRRA) [12]. In order to input the excitation levels in Table 2 as tabular data, the displacement levels were converted into acceleration levels.

This process is shown in Equation (1), which clarifies the influence of system frequency and displacement on acceleration through calculation. Considering the contact characteristics between the cabinet and the isolation table, frictional contact conditions were applied. Since all components are made of SS400, the standard coefficient of friction for structural carbon steel was set at 0.42.

The isolation table is configured in an LM guide format, and a spring is included when combined with the cabinet. This spring shifts the natural frequency into a lower frequency range, improving vibration control performance and absorbing external shocks to reduce the force transmitted to the structure. The LM guide, together with a pair of springs, plays an important role in vibration control and structural stability.

It permits horizontal movement in response to external loads or vibrations while preventing unnecessary rotation and suppressing torsional effects. In the proposed model, a total of eight LM guides were applied, resulting in sixteen springs. The MR damper is a semi-active vibration control device that adjusts its damping force variably by utilizing changes in the viscosity of magneto-rheological fluid under an applied current.

Working in conjunction with the LM guides, the MR damper provides additional damping to effectively suppress residual vibrations. In this study, the MR damper was installed at the position shown in Figure 3(b) to counteract moment effects [13]. The geometry of the LM guide, the rail configuration, and the layout of the damping components are illustrated in Figure 3.

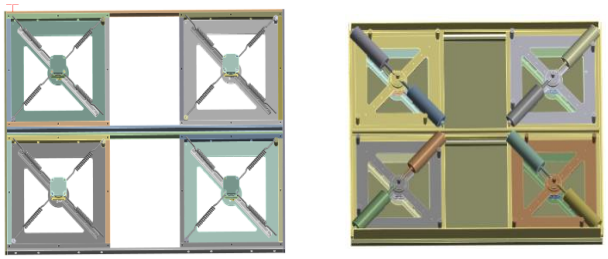

(a) (b)

Fig. 3 Layout of LM guide and damping system (a) LM guide table, and (b) LM guide & MR damper table.

3. Analysis Results

Based on the finite element analysis results, this study conducted simulations by dividing the isolation table structure into three distinct cases. For each case, responses were collected and analyzed in the x- and y-directions at four locations: the top and bottom of the cabinet and the top and bottom of the isolation table, as illustrated in Figure 4. These results were then compared with actual experimental data to verify the reliability of the analysis model. Here, the top of the isolation table refers to the interface where the bottom surface of the cabinet contacts the top surface of the excitation platform.

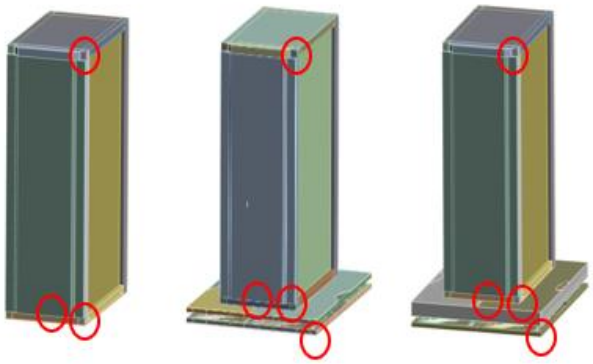

Fig. 4 Response locations

For the isolation table with both the LM guide and MR damper applied, the damping ratio was varied from 0.1 to 0.4, and analysis was conducted accordingly to determine the optimal damping ratio. The analysis results were organized in a table format to enable comparison of the response characteristics for each case.

Table 3. Natural frequencies by mode

Mode	Case 1	Case 2	Case 3
	Frequency (Hz)	Frequency (Hz)	Frequency (Hz)
1	3.6841	0.4896	0.4715
2	9.9668	0.5068	0.4951
3	32.452	0.7593	1.5874
4	32.705	5.0755	4.1471
5	34.539	6.7166	8.3033

Table 3 presents the comparison of natural frequencies for each case. Case 1, in which no isolation system was applied, exhibited relatively high natural frequencies of 3.68 Hz for the first mode and 9.96 Hz for the second mode. In Case 2, where an LM guide was applied, the natural frequencies were 0.48 Hz and 0.50 Hz for the first and second modes, respectively, which represent reductions of more than 86% compared to Case 1, thereby revealing the isolation effect. Case 3, in which both the LM guide and the MR damper were applied, exhibited the lowest natural frequencies among the three cases, with 0.47 Hz for the first mode and 0.49 Hz for the second mode, indicating superior vibration control performance.

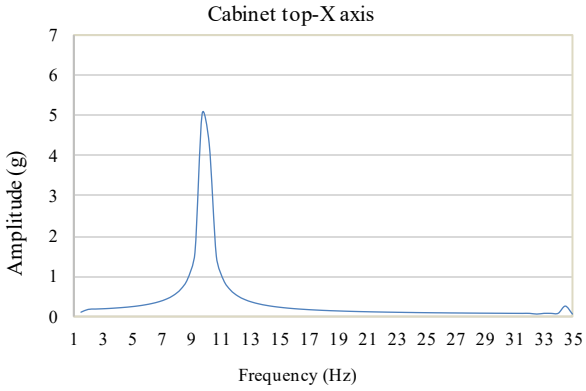

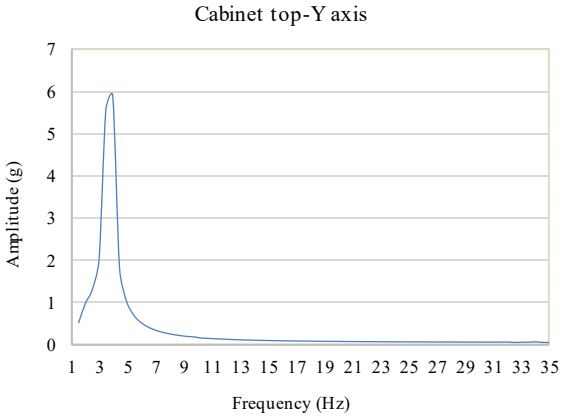

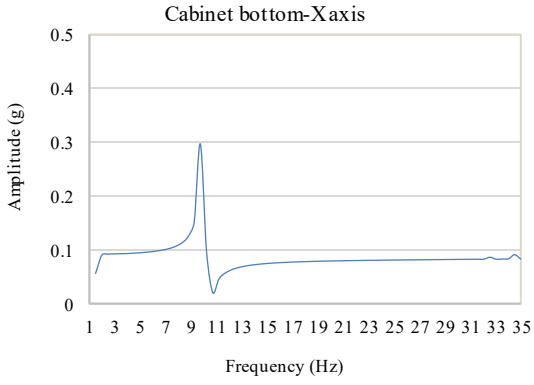

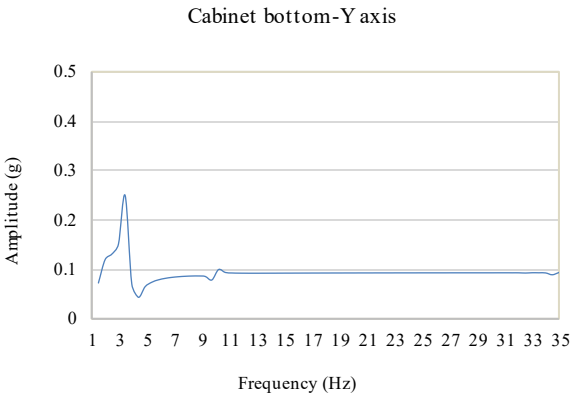

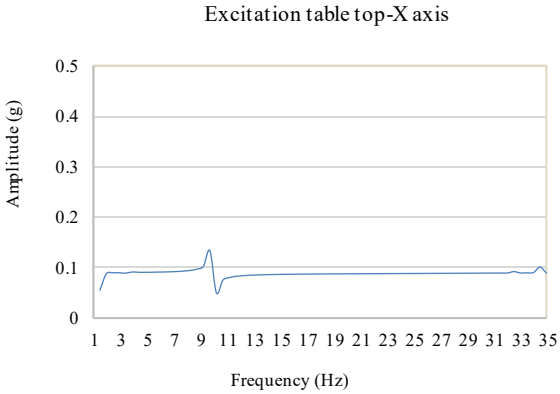

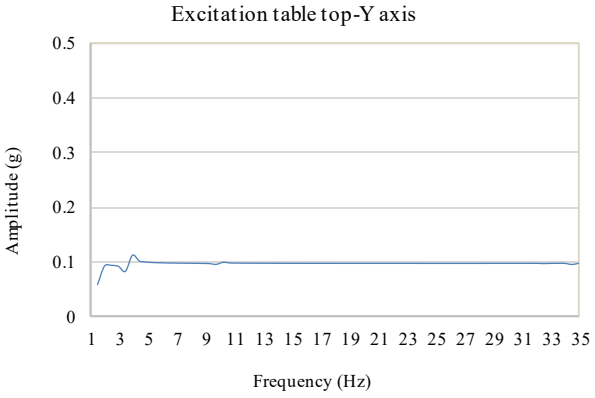

Case 1

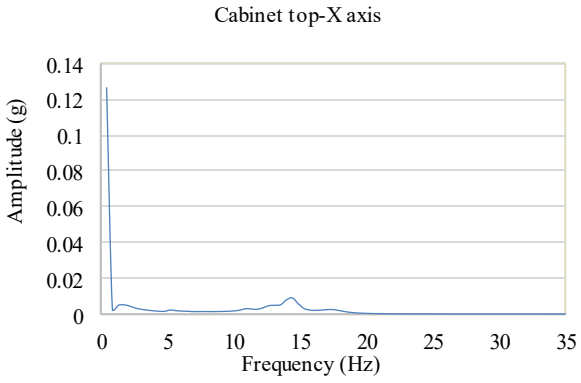

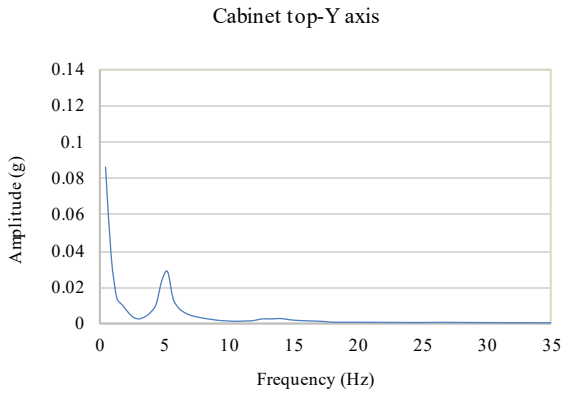
Cabinet top-Y axis
Amplitude (g)
0.14
0.12
0.1
0.08
0.06
0.04
0.02
0
0 5 10 15 20 25 30 35
Frequency (Hz)

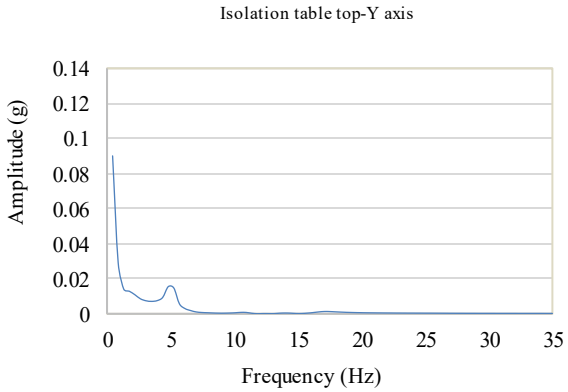
Isolation table top-Y axis
Amplitude (g)
0.14
0.12
0.1
0.08
0.06
0.04
0.02
0
0 5 10 15 20 25 30 35
Frequency (Hz)

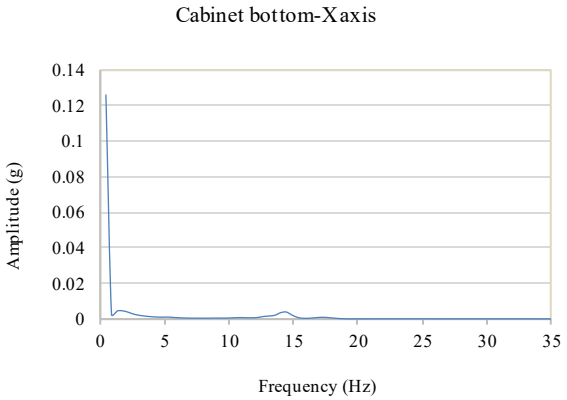
Cabinet bottom-X axis
Amplitude (g)
0.14
0.12
0.1
0.08
0.06
0.04
0.02
0
0 5 10 15 20 25 30 35
Frequency (Hz)

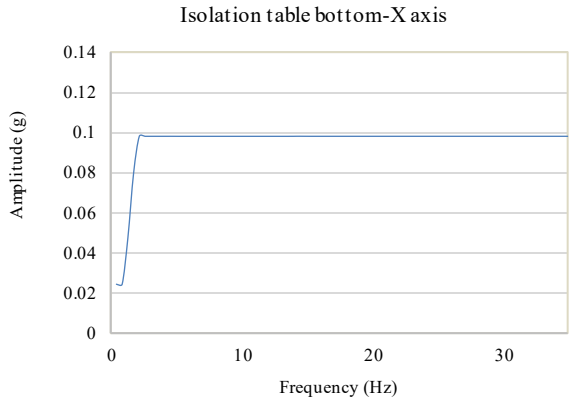
Isolation table bottom-X axis
Amplitude (g)
0.14
0.12
0.1
0.08
0.06
0.04
0.02
0
0 10 20 30
Frequency (Hz)

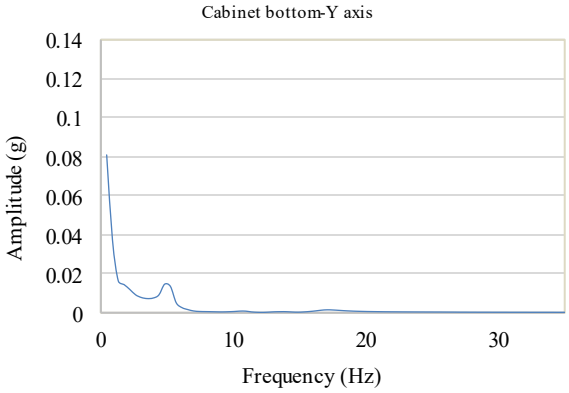
Cabinet bottom-Y axis
Amplitude (g)
0.14
0.12
0.1
0.08
0.06
0.04
0.02
0
0 10 20 30
Frequency (Hz)

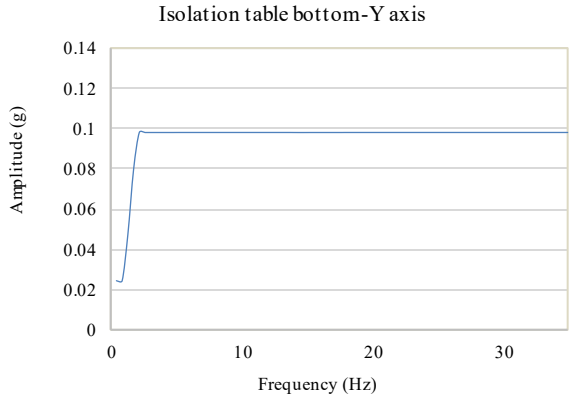
Isolation table bottom-Y axis
Amplitude (g)
0.14
0.12
0.1
0.08
0.06
0.04
0.02
0
0 10 20 30
Frequency (Hz)

Case 2

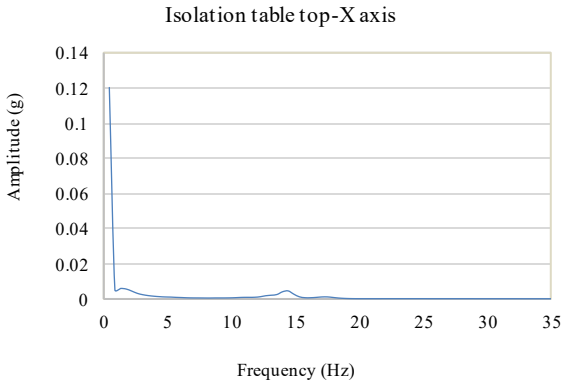
Isolation table top-X axis
Amplitude (g)
0.14
0.12
0.1
0.08
0.06
0.04
0.02
0
0 5 10 15 20 25 30 35
Frequency (Hz)

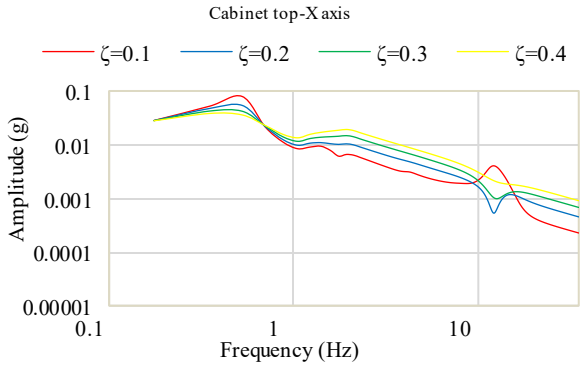
Cabinet top-X axis
ζ=0.1
ζ=0.2
ζ=0.3
ζ=0.4
Amplitude (g)
0.1
0.01
0.001
0.0001
0.00001
0.1 1 10
Frequency (Hz)

Cabinet top-Y axis

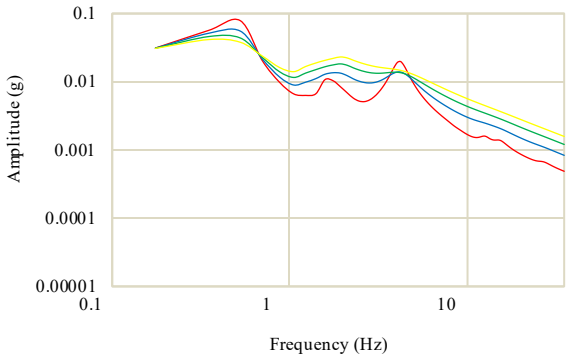

Isolation table top-Y axis

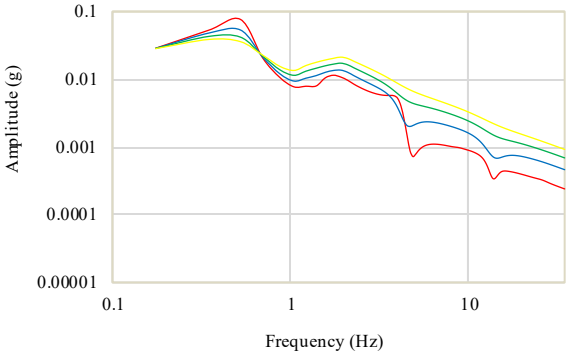

Cabinet bottom-X axis

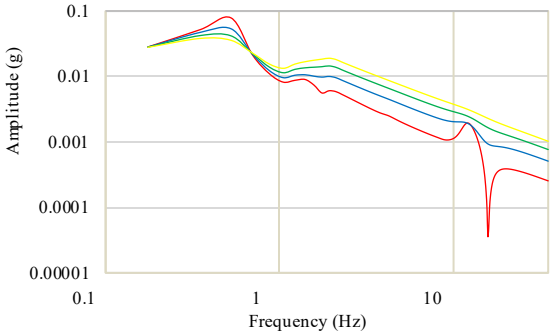

Isolation table bottom-X axis(0.1)

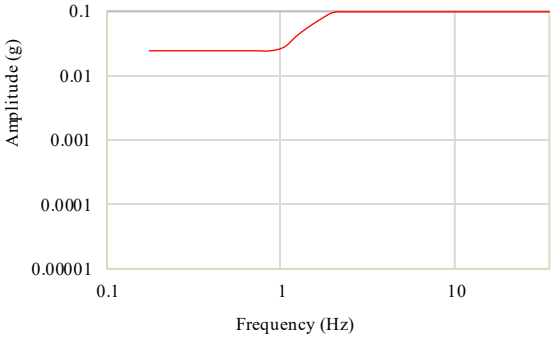

Cabinet bottom-Y axis

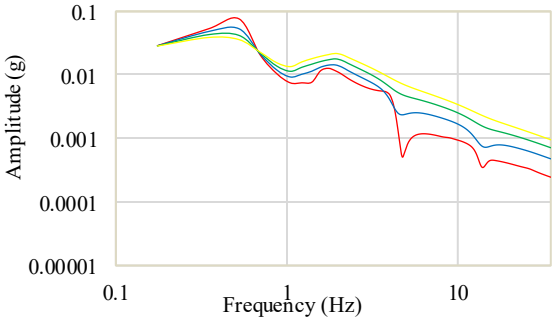

Isolation table bottom-X axis(0.2)

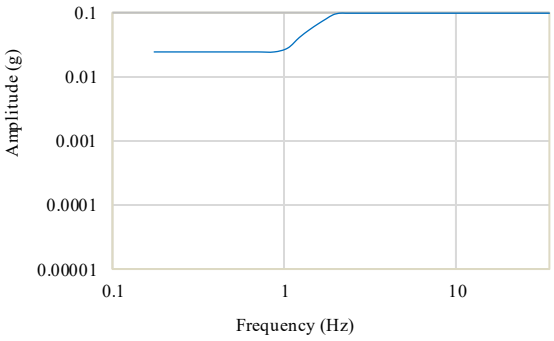

Isolation table top-X axis

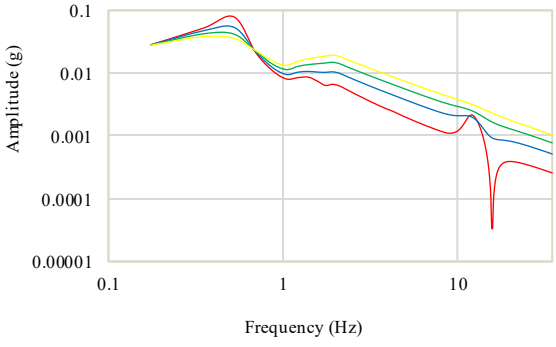

Isolation table bottom-X axis(0.3)

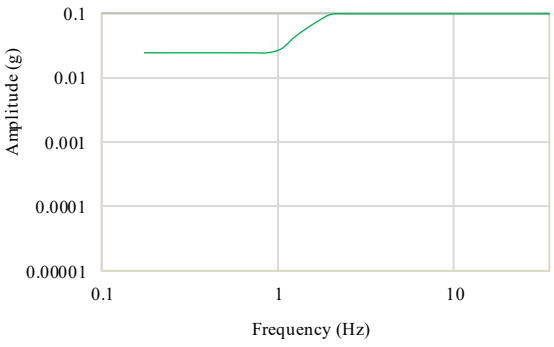

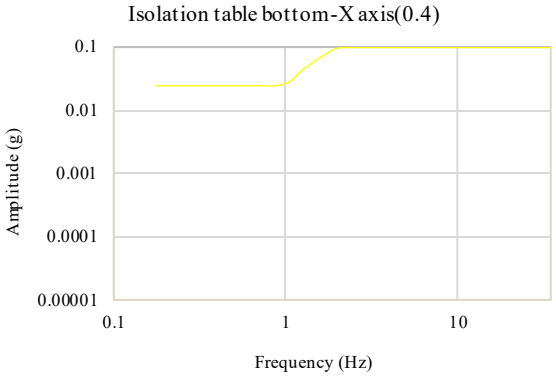

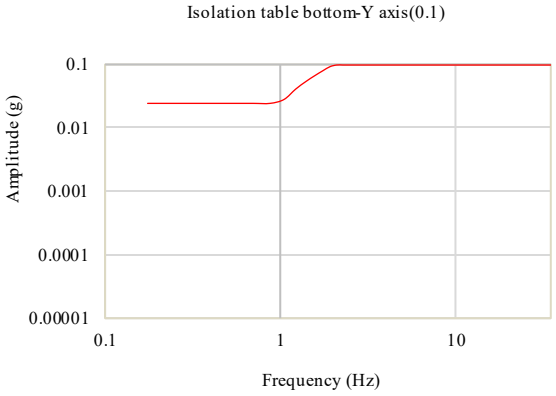

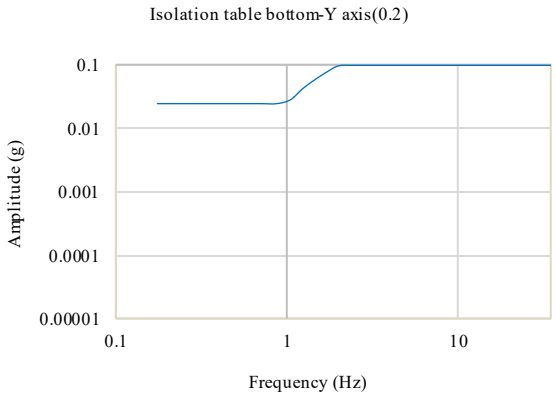

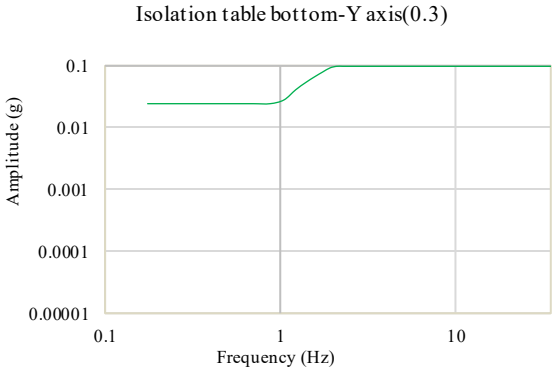

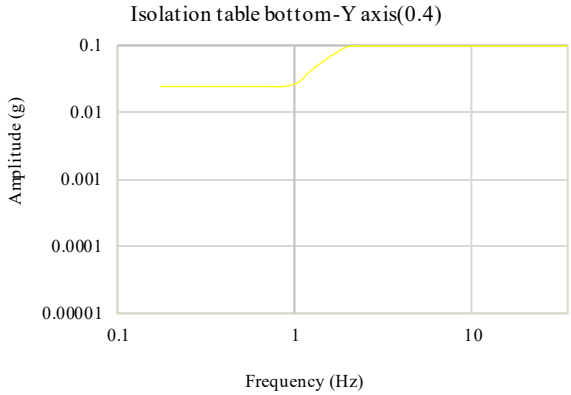

Case 3

Fig. 5 Amplitude response by frequency

Following the natural frequency analysis, the frequency response results are presented in Figure 5. Compared to Case 1, where no isolation system is applied, Cases 2 and 3 showed a significant overall reduction in amplitude.

In particular, Case 3, which includes the MR damper, exhibited the lowest response amplitude, consistent with the results of the dynamic characteristics analysis. When the damping ratio was set to 0.4, the response amplitude approached nearly zero. This suggests that a damping ratio of 0.4 provides optimal vibration reduction, effectively balancing between underdamping and overdamping.

According to vibration isolation theory, when external excitation is applied to a system, the damping effect becomes more pronounced at frequencies higher than the system's natural frequency. Specifically, when the frequency ratio exceeds √2, the transmissibility drops below 1, entering a region where the input vibration is no longer transmitted but instead suppressed. This phenomenon is referred to as vibration isolation. As the frequency ratio increases, the influence of the damping ratio becomes more significant. The transmissibility can be expressed by the following Equation: f is the excitation frequency, fn is the natural frequency, and ζ is the damping ratio.

$$TR = \frac{\sqrt{1+[2\zeta(f/f_n)]^2}}{\sqrt{[1-(f/f_n)^2]^2+[2\zeta(f/f_n)]^2}} \quad (2)$$

This study compared response spectra in the x-axis and y-axis directions as the damping ratio was varied across 0.1, 0.2, 0.3, and 0.4. The analysis results commonly revealed that the first resonance frequency appeared at 0.66 Hz, with notable vibration response characteristics observed at 11.9 Hz in the x-axis and 4.2 Hz in the y-axis.

In particular, in regions where the frequency exceeded √2 times the natural frequency, a clear reduction in amplitude was observed as the damping ratio increased. This trend aligns with the theoretically predicted vibration isolation zone and

serves as an important design guideline for actual system design and the development of vibration mitigation strategies. This corresponds to the theoretically predicted vibration isolation region and serves as an important design criterion in the development of practical systems and vibration mitigation strategies.

4. Conclusion

In this study, to analyze the vibration response characteristics resulting from the application of a base isolation system, a smart isolation device combining an LM guide-based isolation table and an MR damper was proposed and applied to a cabinet system through finite element analysis. The comparison of natural frequencies and frequency response across three models (Case 1: no isolation applied, Case 2: LM guide applied, Case 3: LM guide + MR damper applied) revealed that the application of the isolation system led to a reduction in amplitude and a lowering of natural frequencies. Notably, when the damping ratio was 0.4 in a structure combining an MR damper with an LM guide-based seismic isolation structure, the response amplitude was minimized, indicating effective vibration control. These results demonstrate that the proposed smart isolation system can effectively enhance the vibration stability of critical internal equipment such as communication cabinets. If in future studies, the performance of the proposed system in reducing vibrations of various non-structural components is more quantitatively demonstrated through analytical and experimental methods, it is expected to serve as a design reference for improving seismic performance and disaster response in the future.

References

[1] Yongqing Jiang et al., "A Data-Driven Approach for Predicting Peak Floor Response based on Visually Observed Rocking Behaviors of Freestanding NSCs," *Engineering Structures*, vol. 332, 2025. [CrossRef] [Google Scholar] [Publisher Link]

[2] Myeong Won Seo, Seung-Bok Choi, and Cheol-Ho Kim, "Design and Performance Evaluation of Magnetorheological Damper for Integrated Seismic Isolation System," *Journal of the Korea Academia-Industrial Cooperation Society*, vol. 25, no. 5, pp. 392-398, 2024. [CrossRef] [Google Scholar] [Publisher Link]

[3] Jae Seung Hwang, Seok Jun Joo, and Yun Seok Kim, Kurabayashi, "Dynamic Characteristics and Isolation Performance of Isolation Table System," *Journal of the Earthquake Engineering Society of Korea*, vol. 5, no. 4, pp. 67-74, 2001. [Publisher Link]

[4] Hyun Su Kim, and P.N. Roschke, "Numerical Study of Hybrid Base-Isolator with Magnetorheological Damper and Friction Pendulum System," *Journal of the Earthquake Engineering Society of Korea*, vol. 9, no. 2, pp. 7-15, 2005. [CrossRef] [Google Scholar] [Publisher Link]

[5] Mahdi Abdeddaim et al., "Optimal Design of Magnetorheological Damper for Seismic Response Reduction of Base-Isolated Structures Considering Soil-Structure Interaction," *Structures*, vol. 38, pp. 733-752, 2022. [CrossRef] [Google Scholar] [Publisher Link]

[6] M.D. Christie et al., "A Variable Resonance Magnetorheological-Fluid-Based Pendulum Tuned Mass Damper for Seismic Vibration Suppression," *Mechanical Systems and Signal Processing*, vol. 116, pp. 530-544, 2019. [CrossRef] [Google Scholar] [Publisher Link]

[7] Young-Soo Chun et al., "Seismic Response of Apartment Building with Base Isolation System Consisting of Sliding-Type Bearing and Lead Rubber Bearing," *Journal of the Korea Concrete Institute*, vol. 19, no. 4, pp. 507-514, 2007. [CrossRef] [Google Scholar] [Publisher Link]

[8] Yerik T. Bessimbayev et al., "The Creation of Geotechnical Seismic Isolation from Materials with Damping Properties for the Protection of Architectural Monuments," *Buildings*, vol. 14, no. 5, pp. 1-17, 2024. [CrossRef] [Google Scholar] [Publisher Link]

[9] Pan Liu et al., "Seismic Performance of Hybrid Seismic Isolation Bearing System: Shake Table Test and Nonlinear Numerical Analysis," *Soil Dynamics and Earthquake Engineering*, vol. 196, 2025. [CrossRef] [Google Scholar] [Publisher Link]

[10] Chieh-Yu Liu, and Chio-Ming Chang, "Design and Performance Evaluation of Seismic Isolation Bearings with Oblique Viscous Damper for Protection of Essential Equipment and Components," *Engineering Structures*, vol. 336, 2025. [CrossRef] [Google Scholar] [Publisher Link]

[11] Yiyang Wei et al., "A New Sliding Three-Dimensional Seismic Isolation Bearing Mechanical Model and its Seismic Performance," *Structures*, vol. 72, 2025. [CrossRef] [Google Scholar] [Publisher Link]

[12] Saebyeok Jeong et al., "Dynamic Responses of Base Isolation Devices for Telecommunication Equipment in Building Structures," *Journal of the Korea Institute for Structural Maintenance and Inspection*, vol. 26, no. 1, pp. 39-48, 2022. [CrossRef] [Google Scholar] [Publisher Link]

[13] Sang-Won Cho et al., "Smart Passive System Based on MR Damper," *Journal of the Earthquake Engineering Society of Korea*, vol. 9, no.1, pp. 51-59, 2005. [CrossRef] [Google Scholar] [Publisher Link]